

# Fully Solution-Processed Low-Voltage Aqueous In<sub>2</sub>O<sub>3</sub> Thin-Film Transistors Using an Ultrathin ZrO<sub>x</sub> Dielectric

Ao Liu,<sup>†</sup> Guo Xia Liu,<sup>†</sup> Hui Hui Zhu,<sup>†</sup> Feng Xu,<sup>†</sup> Elvira Fortunato,<sup>‡</sup> Rodrigo Martins,<sup>‡</sup> and Fu Kai Shan<sup>\*†</sup>

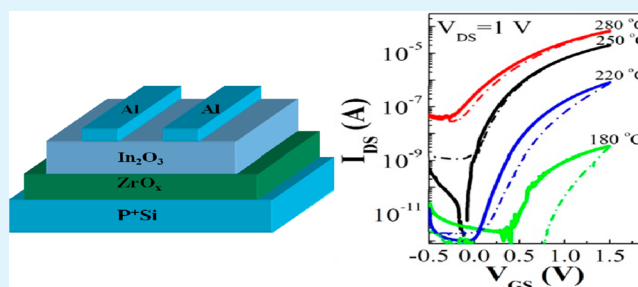
<sup>†</sup>College of Physics and Lab of New Fiber Materials and Modern Textile, Growing Base for State Key Laboratory, Qingdao University, Qingdao 266071, China

<sup>‡</sup>Department of Materials Science/CENIMAT-I3N, Faculty of Sciences and Technology, New University of Lisbon and CEMOP-UNINOVA, Campus de Caparica, 2829-516 Caparica, Portugal

## Supporting Information

**ABSTRACT:** We reported here “aqueous-route” fabrication of In<sub>2</sub>O<sub>3</sub> thin-film transistors (TFTs) using an ultrathin solution-processed ZrO<sub>x</sub> dielectric thin film. The formation and properties of In<sub>2</sub>O<sub>3</sub> thin films under various annealing temperatures were intensively examined by thermogravimetric analysis, Fourier transform infrared spectroscopy, and atomic force microscopy. The solution-processed ZrO<sub>x</sub> thin film followed by sequential UV/ozone treatment and low-temperature thermal-annealing processes showed an amorphous structure, a low leakage-current density ( $\sim 1 \times 10^{-9}$  A/cm<sup>2</sup> at 2 MV/cm), and a high breakdown electric field ( $\sim 7.2$  MV/cm). On the basis of its implementation as the gate insulator, the In<sub>2</sub>O<sub>3</sub> TFTs based on ZrO<sub>x</sub> annealed at 250 °C exhibit an on/off current ratio larger than 10<sup>7</sup>, a field-effect mobility of 23.6 cm<sup>2</sup>/V·s, a subthreshold swing of 90 mV/decade, a threshold voltage of 0.13 V, and high stability. These promising properties were obtained at a low operating voltage of 1.5 V. These results suggest that “aqueous-route” In<sub>2</sub>O<sub>3</sub> TFTs based on a solution-processed ZrO<sub>x</sub> dielectric could potentially be used for low-cost, low-temperature-processing, high-performance, and flexible devices.

**KEYWORDS:** aqueous solution process, low-temperature process, ultrathin zirconium oxide, indium oxide, thin-film transistor



Amorphous metal oxide semiconductors have been extensively studied as the channel materials for thin-film transistors (TFTs) in display backplanes and other optoelectronic devices.<sup>1,2</sup> Recently reported electrical parameters of metal oxide TFTs, especially the carrier mobility, are generally superior to those of amorphous silicon-based TFTs and, in some cases, even comparable to those of polycrystalline silicon-based TFTs.<sup>3,4</sup> However, these TFTs were typically manufactured by vacuum-based methods. Although the vacuum-based deposition methods have their own advantages, the high fabrication cost and large-area device uniformity restrict the areas of their applications.<sup>5</sup> For this consideration, considerable researches have been conducted on the development of a solution process for the construction of metal oxide TFTs.<sup>5–7</sup> It is noted that, in most of the previous reports of solution-processed TFTs, a high-temperature annealing process is imperative to achieving reasonable electrical properties. To decrease the annealing temperature of solution-processed oxide layers, several research groups have proposed novel approaches to achieve oxide TFTs at temperatures under 300 °C, including sol–gel on chip,<sup>8</sup> a chemical energetic combustion process through an oxidizer and fuel,<sup>9</sup> a UV/ozone photoannealing method,<sup>10</sup> annealing in an O<sub>2</sub>/O<sub>3</sub> atmospheric environment,<sup>11</sup> and zinc hydroxamine complex precursors.<sup>12</sup> However, most of these approaches fabricated the TFTs on thermally grown or

vacuum-deposited SiO<sub>2</sub> dielectrics, which will certainly result in high operating voltages (larger than 40 V).

It is known that the use of appropriate solvents, metal precursors, and gate dielectrics is crucial to enable low processing temperature and high device performances. Park et al. proposed an “aqueous route” to fabricate metal oxide TFTs with the maximum processing temperature not exceeding 350 °C.<sup>6</sup> Because water is used as a solvent, instead of the often-used 2-methoxyethanol (2-ME)-based organic solvents, the “aqueous-route” synthesis is considered to be healthier, safer, and environmentally friendlier. Unlike several conventionally used 2-ME-based precursors, the aqueous solutions are insensitive to ambient moisture. The inert atmosphere to store and handle a precursor solution is not necessary.<sup>13</sup> More importantly, because the coordinating bond between the metal cation and neighboring aquo ion is relatively weak (electrostatic interaction), it is easily broken with low thermal energy compared with the covalent bonds in the 2-ME-based precursor.<sup>5</sup> Therefore, “aqueous route” is considered to be a promising technique to fabricate the metal oxide layers at low temperature.

Received: August 20, 2014

Accepted: October 3, 2014

Published: October 6, 2014

As a candidate of channel material, indium oxide ( $\text{In}_2\text{O}_3$ ) has been widely studied because it can provide high electron mobility originating from the ns orbital of indium. The ns orbital is larger than the 2p orbital of the oxygen anion.<sup>1,14</sup> Meanwhile,  $\text{In}_2\text{O}_3$  is one of the semiconductor materials that can be achieved by the solution process and exhibits various electrical performances depending on the stoichiometry and defects in materials.<sup>11</sup> When the advantages of “aqueous route” and  $\text{In}_2\text{O}_3$  materials are combined, aqueous  $\text{In}_2\text{O}_3$  is considered to be an ideal candidate to fabricate the high-mobility channel layer for TFT devices at low temperature.

Moreover, the gate dielectric plays an equally critical role in determining the electrical performances of the oxide TFTs. Generally, gate dielectrics are required to be smooth, dense, and pinhole-free to allow a low leakage current and a high breakdown electric field.<sup>7</sup> However, for metal oxide dielectrics fabricated at low temperature (<300 °C), it is difficult to achieve the aforementioned purposes.<sup>14,15</sup> In our previous report, a UV/ozone-treated  $\text{ZrO}_x$  dielectric thin film was successfully fabricated to replace  $\text{SiO}_2$  as the dielectric for  $\text{InTiZnO}$  TFTs.<sup>16</sup> The smooth surface and excellent electrical performances of the  $\text{ZrO}_x$  dielectric guaranteed that the as-fabricated TFTs exhibited decent characteristics at a low operating voltage of 3 V.

On the basis of our previous solution process for oxide dielectrics, we further demonstrate the fabrication of high-performance and low-operating-voltage TFTs using aqueous  $\text{In}_2\text{O}_3$  as channel layers. The effects of the annealing temperature on the thermal behavior, chemical properties, surface morphologies, and performances of the TFT devices were also studied.

The detailed experimental section and instrumental analysis are shown in sections S1 and S2 in the Supporting Information (SI). To understand the thermal behaviors of  $\text{ZrO}_x$  and  $\text{In}_2\text{O}_3$  precursor solutions, thermogravimetric analysis (TGA) measurements were performed, and the results are shown in Figure 1. In general, the hydrolysis reaction of precursor xerogel occurred in the temperature range of 100–150 °C.<sup>6</sup> In this experiment, because the indium precursor was dissolved in water, the ionized indium cation was solvated by the neighboring water molecules. Because the coordination number of  $\text{In}^{3+}$  was 6, it was considered to be a true coordination

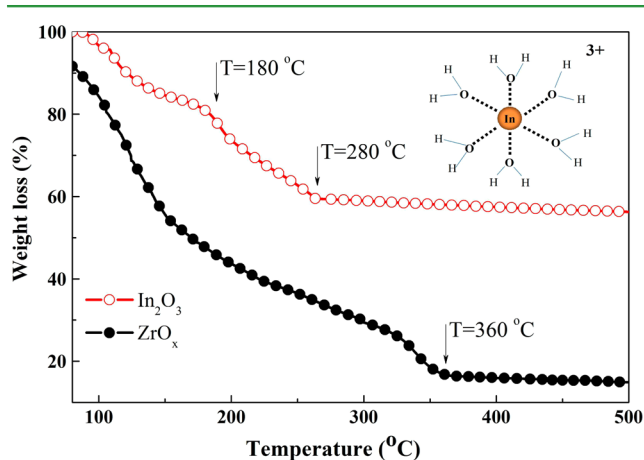


**Figure 1.** Thermal behaviors of  $\text{In}_2\text{O}_3$  and  $\text{ZrO}_x$  dried precursor solutions. The inset represents the proposed indium complex in aqueous solution.

complex, with six water molecules acting as  $\sigma$ -donating ligands.<sup>13</sup> For  $\text{In}_2\text{O}_3$  xerogel, dehydroxylation of indium hydroxide began at  $\sim 180$  °C and was nearly complete when the xerogel was annealed at temperatures higher than 280 °C. On the basis of this dehydroxylation behavior, the annealing condition for aqueous  $\text{In}_2\text{O}_3$  thin films was estimated to be from 180 to 280 °C. For  $\text{ZrO}_x$  xerogel, no significant weight loss was observed at temperatures above 360 °C. In the previously reported literature, UV/ozone treatment has been proven to be effective in decreasing the decomposition temperature for metal oxide thin films.<sup>10,17</sup> However, there have been no reports applying this technique to fabricate the dielectrics. In this work, a  $\text{ZrO}_x$  dielectric was processed using a UV/ozone pretreatment before the thermal-annealing process. Meanwhile, in order to reduce the thermal budget (indium diffusion and miscibility phenomenon) brought by the annealing treatment for  $\text{In}_2\text{O}_3$  channel layers and to guarantee a low-temperature process, we conducted the annealing process for a  $\text{ZrO}_x$  dielectric at 300 °C.

To better understand the formation of  $\text{In}_2\text{O}_3$  thin films with aforementioned annealing conditions, Fourier transform infrared (FT-IR) measurements were carried out, and the results are shown in Figure 2. Several vibration peaks are observed in the

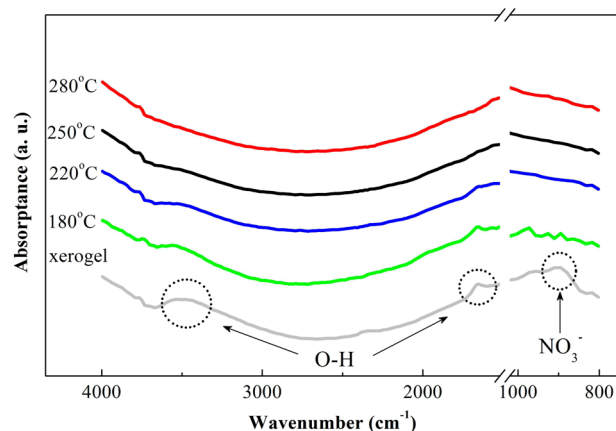


**Figure 2.** FT-IR spectra of the  $\text{In}_2\text{O}_3$  thin films annealed at different temperatures.

$\text{In}_2\text{O}_3$  xerogel film. The broad peaks in the ranges of 3300–3500 and 1500–1700  $\text{cm}^{-1}$  indicate O–H stretching vibrations.<sup>6</sup> The peak at 850  $\text{cm}^{-1}$  is related to the existence of  $\text{NO}_3^-$ .<sup>18</sup> As the annealing temperature was increased to 180 °C, the nitrate groups were pyrolyzed, while a large amount of hydroxyl species still remained in the thin films. In the case of annealing temperatures higher than 250 °C, the O–H vibration peaks disappeared, and the spectrum was similar to that of the substrate. This indicated that the metal hydroxides  $[\text{In}(\text{OH})_2]_6^{3+}$  were converted to metal oxides ( $\text{In}_2\text{O}_3$ ). In view of the TGA and FT-IR results, it was proven that the weight loss in the temperature range of 80–180 °C mainly originated from the decomposition of nitrate groups and the continuous decrease was caused by the dehydroxylation reaction.

Parts a and b of Figure 3 show the atomic force microscopy (AFM) image of a  $\text{ZrO}_x$  thin film and the root-mean-square (RMS) values of  $\text{In}_2\text{O}_3$  thin films on  $\text{ZrO}_x$  annealed at different temperatures, respectively. The X-ray diffraction (XRD) patterns of various  $\text{In}_2\text{O}_3$  thin films are shown in Figure S1 in the SI. The  $\text{ZrO}_x$  thin film exhibits a smooth surface with a

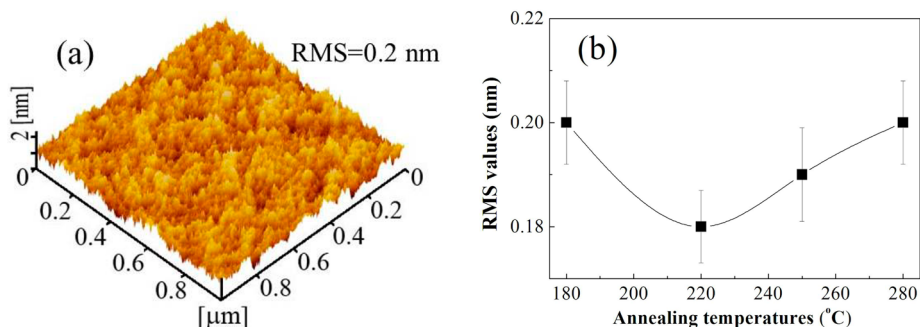


**Figure 3.** (a) AFM image of a  $\text{ZrO}_x$  thin film. (b) RMS values of  $\text{In}_2\text{O}_3$  thin films on  $\text{ZrO}_x$  annealed at different annealing temperatures.

roughness of 0.2 nm and free pinholes. Prior to the thermal-annealing process, the UV/ozone treatment allowed the volatile gases, originally from solvent, to overflow slowly through the surface of the gel thin films. Therefore, the surface of the  $\text{ZrO}_x$  thin film with a UV/ozone pretreatment was kept as smooth as possible. A smooth surface is beneficial for charge-carrier transportation in semiconductors because a rough interface could induce physical traps or disturb the growth of channel layers. The average RMS values of  $\text{In}_2\text{O}_3$  thin films on  $\text{ZrO}_x$  annealed at various temperatures were measured as 0.20, 0.18, 0.19, and 0.20 nm, respectively. These small surface roughness values are beneficial from the smooth surface of the  $\text{ZrO}_x$  thin film and are ideal for obtaining a high device performance.

To characterize the dielectric and electrical properties of the  $\text{ZrO}_x$  thin films, a capacitor with the structure of  $\text{Al}/\text{ZrO}_x/\text{p}^+\text{-Si}$  was employed. Figure 4 shows the areal capacitance of the  $\text{ZrO}_x$

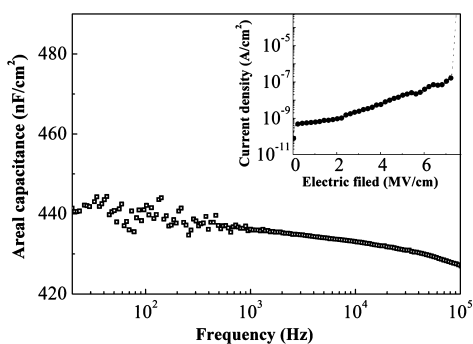


**Figure 4.** Areal capacitance and dielectric constant of an  $\text{Al}/\text{ZrO}_x/\text{p}^+\text{-Si}$  capacitor as a function of the frequency. The leakage-current density versus electric field is shown in the inset.

capacitor in the frequency range between 20 Hz ( $440 \text{ nF}/\text{cm}^2$ ) and 100 kHz ( $426 \text{ nF}/\text{cm}^2$ ). Such a large capacitance density can effectively decrease the operating and subthreshold voltages of the TFT devices. In addition, the  $\text{ZrO}_x$  dielectric showed a small frequency dispersion of the capacitance ( $\sim 3.2\%$ ), indicating a low defect density such as hydroxyl group and/or oxygen vacancies in the thin film.<sup>19</sup> This is undoubtedly beneficial to the leakage current because the conduction paths in dielectrics are mainly caused by hydroxyl and grain boundaries. During the fabrication of high- $k$  dielectrics on a silicon wafer using chemical methods, the presence of  $\text{SiO}_2$  interface layer (IL) can cause a decrease of the  $k$  value. In order to calculate the dielectric constant of the  $\text{ZrO}_x$  thin film, the influence of the  $\text{SiO}_2$  IL between  $\text{ZrO}_x$  and the silicon wafer must be excluded. Assuming that the IL is  $\text{SiO}_2$ , the effective dielectric constant, estimated using a series capacitor model ( $1/$

$C_{\text{SiO}_2} + 1/C_{\text{ZrO}_2} = 1/C_{\text{total}}$ ), was calculated to be around 12.5. The inset of Figure 4 presents the leakage-current density ( $J_{\text{leak}}$ ) of the  $\text{ZrO}_x$  capacitor at various electric fields. The capacitor exhibits a low  $J_{\text{leak}}$  of  $1 \times 10^{-9} \text{ A}/\text{cm}^2$  at  $2.0 \text{ MV}/\text{cm}$  and a high dielectric breakdown electric field of  $7.2 \text{ MV}/\text{cm}$ .  $J_{\text{leak}}$  is nearly 2 orders of magnitude smaller than the previously published results of the sol-gel-derived  $\text{ZrO}_x$  dielectrics that were annealed at  $300 \text{ }^\circ\text{C}$  or were treated by UV/ozone.<sup>20,21</sup> The low leakage-current density and high breakdown electric field are due to not only the smooth surface, dense structure, and high oxidation states of the  $\text{ZrO}_x$  thin film but also its amorphous structure (shown in Figure S2 in the SI). All of the properties suggest that the UV/ozone treatment followed by a low-temperature annealing process have great potential for the gate dielectrics in fabricating the low-voltage, high-performance oxide TFTs.

To investigate the performance of aqueous  $\text{In}_2\text{O}_3$  TFTs integrated on solution-processed high- $k$   $\text{ZrO}_x$  dielectric, TFT devices with bottom-gate and top-contact architecture were fabricated. The output curves are shown in Figure S3 in the SI, and the summarized output curves of the  $\text{In}_2\text{O}_3$  TFTs at a  $V_{\text{GS}}$  of  $1.5 \text{ V}$  are depicted in Figure 5a. These devices exhibit typical n-channel behavior with clear pinch-off voltage and current saturation. It can be seen that the operating voltage is only  $1.5 \text{ V}$ , which is important for low-power electronics. Figure 5b shows the corresponding transfer characteristics of  $\text{In}_2\text{O}_3$  TFTs with a double-sweep gate voltage model. All of these TFTs show hysteresis characteristics, and their direction is clockwise. When the annealing temperature was  $180 \text{ }^\circ\text{C}$ , the device exhibited poor performance, including a low saturation current of  $3 \times 10^{-9} \text{ A}$  and a large hysteresis behavior with a  $0.34 \text{ V}$  voltage shift. The large hysteresis window and low saturation currents are mainly due to the number of defect states and the degree of oxidation in the semiconductor channel layers.<sup>22</sup> According to the results of FT-IR, the incomplete decomposition of nitrate groups and large amounts of hydroxide undoubtedly degraded the performance of the TFT device. With the accelerated dehydroxylation reaction and the formation of In–O bonds in  $\text{In}_2\text{O}_3$  channel layers at higher annealing temperatures, the saturation current increased from  $8.5 \times 10^{-7} \text{ A}$  ( $220 \text{ }^\circ\text{C}$ ) to  $8.7 \times 10^{-5} \text{ A}$  ( $280 \text{ }^\circ\text{C}$ ) and hysteresis windows became negligible.

To further investigate the electrical properties of the as-fabricated  $\text{In}_2\text{O}_3$  TFTs, the threshold voltage ( $V_{\text{TH}}$ ) was defined by fitting a straight line to the plot of the square root of  $I_{\text{DS}}$  versus  $V_{\text{GS}}$ . The field-effect mobility ( $\mu_{\text{FE}}$ ) can be calculated in the saturation region ( $V_{\text{DS}} > V_{\text{G}} - V_{\text{TH}}$ ) using the following equation:



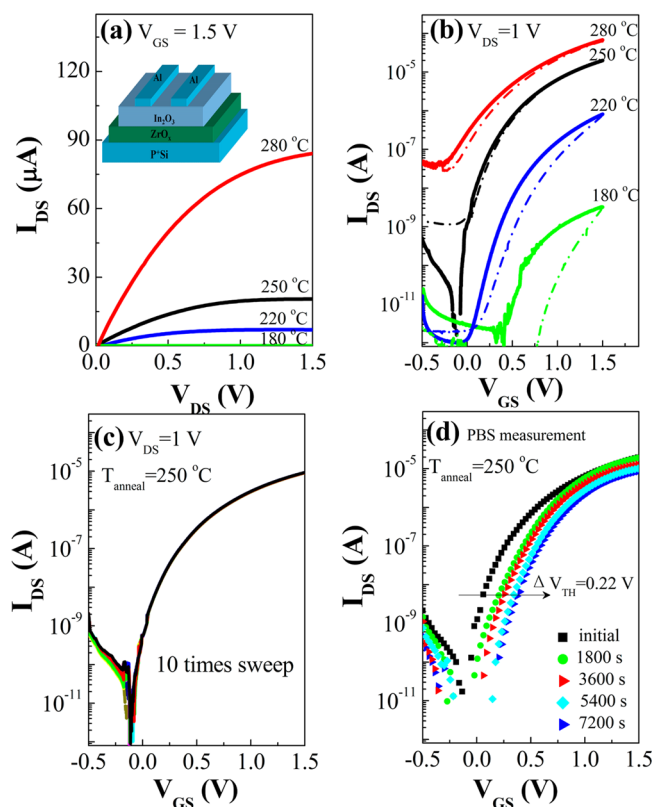


**Figure 5.** (a) Summarized output curves of  $\text{In}_2\text{O}_3$  TFTs on  $\text{ZrO}_x$  annealed at various annealing temperatures. (b) Corresponding transfer characteristics of  $\text{In}_2\text{O}_3$  TFTs at  $V_D = 1$  V as a function of the annealing temperature. (c) 10 times sweep test for a 250 °C annealed  $\text{In}_2\text{O}_3$  TFT. (d) Transfer curves of a 250 °C annealed  $\text{In}_2\text{O}_3$  TFT under PBS with a  $V_{GS}$  value of 1.5 V for 7200 s.

$$I_{DS} = \frac{1}{2} \frac{W}{L} C_i \mu_{FE} (V_{GS} - V_{TH})^2 \quad (1)$$

where  $C_i$ ,  $L$ , and  $W$  are the areal capacitance of the  $\text{ZrO}_x$  dielectric and the channel length and width of the TFT, respectively. The electrical parameters of the TFTs are summarized in Table I. The  $\mu_{FE}$  values of the  $\text{In}_2\text{O}_3$  TFTs annealed at 220, 250, and 280 °C were calculated to be 1.1, 23.6, and 29.5  $\text{cm}^2/\text{V}\cdot\text{s}$ , respectively. It is known that the conduction band minimum (CBM) in metal oxide semiconductors should be primarily composed of dispersed vacant s states with short interaction distances for efficient carrier transportation, which can be achieved in ionic oxide but not obviously in hydroxide.<sup>23</sup> Therefore, the dehydroxylation reaction at higher annealing temperatures for  $\text{In}_2\text{O}_3$  channel layers not only increased the saturation current but also enhanced the  $\mu_{FE}$  value of the as-fabricated TFTs.

It can be clearly seen from Table I that the electrical performance of the  $\text{In}_2\text{O}_3$  TFTs annealed at 250 °C showed the best performance, including a reasonable  $\mu_{FE}$  of 23.6  $\text{cm}^2/\text{V}\cdot\text{s}$ , a

high on/off current ratio ( $I_{on}/I_{off}$ ) of  $1.1 \times 10^7$ , a low  $V_{TH}$  of 0.13 V, and a small subthreshold swing (SS) of 90 mV/dec. Generally, the SS values directly reflect the switching speed and power consumption of the TFT devices. The small SS values for all of these TFTs were beneficial from the large areal capacitance of the  $\text{ZrO}_x$  dielectric and the electronic-clean interface between  $\text{In}_2\text{O}_3$  and  $\text{ZrO}_x$ . Although a high saturation current and large  $\mu_{FE}$  were obtained in the case of the  $\text{In}_2\text{O}_3$  TFT annealed at 280 °C, it was found to operate in the depletion mode with a negative  $V_{TH}$  of  $-0.27$  V because of high carrier concentration arising from the Fermi level proximity to the CBM.<sup>2</sup> The high carrier concentration, together with enhancement of the interface defects in the dielectric channel interface, will make it difficult to deplete the  $\text{In}_2\text{O}_3$  channel layer, leading to a negative  $V_{TH}$ , a high off current, and a low  $I_{on}/I_{off}$  value. On the basis of the results of the  $\text{In}_2\text{O}_3$  TFTs annealed at various temperatures, it can be deduced that appropriate self-doping (especially hydroxyl species) in the  $\text{In}_2\text{O}_3$  system at low temperature is needed to control the excess carrier concentration and to optimize the dielectric/channel interface and so the electrical performances of the TFT devices. To our best knowledge, this is the lowest reported operating voltage for fully solution-processed TFTs. In this study, the aqueous route allows fabrication of the  $\text{In}_2\text{O}_3$  TFTs at much lower temperature compared with the previously reported 2-ME-based approach.<sup>11,24</sup> This result represents a significant step toward the development of nontoxic, low-cost, and large-area oxide electronics.

The degradation behavior of the  $\text{In}_2\text{O}_3$  TFT annealed at 250 °C was also investigated by measuring the  $V_{TH}$  shift in consecutive transfer curves. This simple procedure is useful to analyze the early-stage aging of devices and also to deduce the instability mechanism that might be present.<sup>25</sup> Figure 5c shows the results of a consecutive 10-time sweep test at  $V_D = 1$  V. High stability without any degradation was exhibited in this test. This result can be attributed to two reasons: one is due to the fact that a low density of trap states exists at the  $\text{In}_2\text{O}_3/\text{ZrO}_x$  interface (as indicated in the AFM results); the other is due to the fact that the background carrier concentration in the  $\text{In}_2\text{O}_3$  channel layer is enough to fill the traps at zero-gate bias. Meanwhile, a positive bias stress (PBS) test for a 250 °C annealed  $\text{In}_2\text{O}_3/\text{ZrO}_x$  TFT was performed. The device was stressed under the following conditions:  $V_{GS}$  and  $V_{DS}$  were set to 1.5 and 1.0 V, respectively; the stress duration was 7200 s. The threshold voltage shift ( $\Delta V_{TH}$ ) in the transfer curves under the PBS test is shown in Figure 5d. The parallel  $V_{TH}$  shift of the transfer curve ( $\sim 0.22$  V), with a negligible change in the SS value is considered to be from the carrier-trapping mechanism.<sup>26</sup> The hysteresis measurement and consequence sweep test in transfer curves indicate very few trap defects existing in the 280 °C annealed  $\text{In}_2\text{O}_3$  channel layer and  $\text{In}_2\text{O}_3/\text{ZrO}_x$  interface. Therefore, the charge-trapping model alone cannot entirely account for the results obtained. Jeong et al.<sup>27</sup> and Pan et al.<sup>28</sup> reported that the interaction between the channel layer

**Table I.** Electrical Parameters of  $\text{In}_2\text{O}_3$  TFTs on a  $\text{ZrO}_x$  Dielectric Annealed at Various Temperatures

$\text{In}_2\text{O}_3$ annealing temperature (°C)	$\mu_{FE}$ ( $\text{cm}^2/\text{V}\cdot\text{s}$ )	$I_{on}/I_{off}$	$V_{TH}$ (V)	SS (mV/dec)	hysteresis (V)
180		$10^3$ – $10^4$	$0.71 \pm 0.05$	$160 \pm 15$	$0.41 \pm 0.09$
220	$1.1 \pm 0.4$	$10^5$ – $10^6$	$0.58 \pm 0.03$	$110 \pm 10$	$0.33 \pm 0.05$
250	$23.6 \pm 0.3$	$\sim 10^7$	$0.13 \pm 0.02$	$90 \pm 10$	$0.05 \pm 0.02$
280	$29.5 \pm 0.9$	$10^3$ – $10^4$	$-0.27 \pm 0.06$	$390 \pm 20$	$0.09 \pm 0.03$

and oxygen in an ambient atmosphere plays a critical role in determining the  $V_{\text{TH}}$  instability. When the PBS test was applied in the atmosphere, excess electrons accumulated in the channel layer. The surrounding oxygen molecules have large electron negativity, which can capture electrons from the conduction band to form  $\text{O}^{2-}$  species. The adsorption of oxygen molecules in the channel layer can deplete the electron carriers, leading to a positive shift of  $\Delta V_{\text{TH}}$ .<sup>29</sup>

In summary, we have integrated an aqueous route with solution deposition of oxide-based TFTs. An ultrathin solution-processed  $\text{ZrO}_x$  thin film was fabricated as the dielectric, which was processed by a UV/ozone treatment and a low-temperature annealing process. Such a  $\text{ZrO}_x$  layer exhibited excellent electrical performance as a gate insulator, such as a high dielectric constant of  $\sim 12.5$ , a low leakage-current density of  $1 \times 10^{-9}$  A/cm<sup>2</sup> at 2.0 MV/cm, and a high breakdown electric field of 7.2 MV/cm. The optimized  $\text{In}_2\text{O}_3$  TFT, which was annealed at 250 °C, exhibited high performances with a  $\mu_{\text{FE}}$  of 23.6 cm<sup>2</sup>/V·s, an  $I_{\text{on}}/I_{\text{off}}$  value of  $1.1 \times 10^7$ ,  $V_{\text{TH}}$  of 0.13 V, and SS of 90 mV/decade. All of these decent electrical performances were obtained at a low operating voltage of 1.5 V. The “aqueous route” is applicable to a broad range of amorphous metal oxide compositions, and it should also provide a new approach for integrating more amorphous oxide materials into functional electronic and optoelectronic devices.

## ■ ASSOCIATED CONTENT

### ■ Supporting Information

Experimental section, instrumental analysis, XRD patterns of water-induced  $\text{In}_2\text{O}_3$  thin films annealed at various annealing temperatures and of a  $\text{ZrO}_x$  thin film, output curves of  $\text{In}_2\text{O}_3/\text{ZrO}_x$  TFTs as a function of the annealing temperature, and leakage-current density versus electric field curves of  $\text{ZrO}_x$  thin films annealed at various conditions. This material is available free of charge via the Internet at <http://pubs.acs.org>.

## ■ AUTHOR INFORMATION

### ■ Corresponding Author

\* E-mail: [fkshan@qdu.edu.cn](mailto:fkshan@qdu.edu.cn).

### ■ Notes

The authors declare no competing financial interest.

## ■ ACKNOWLEDGMENTS

This study was supported by the Natural Science Foundation of China (Grant 51472130) and Natural Science Foundation of Shandong Province (Grants ZR2011FM010 and ZR2012FM020) as well as by the Portuguese Science Foundation (FCT-MEC) through Projects EXCL/CTM-NAN/0201/2012 and PEst-C/CTM/LA0025/2013-14.

## ■ REFERENCES

- (1) Nomura, K.; Ohta, H.; Takagi, A.; Kamiya, T.; Hirano, M.; Hosono, H. Room-temperature fabrication of transparent flexible thin-film transistors using amorphous oxide semiconductors. *Nature* **2004**, *432*, 488–492.
- (2) Fortunato, E.; Barquinha, P.; Martins, R. Oxide Semiconductor Thin-Film Transistors: A Review of Recent Advances. *Adv. Mater.* **2012**, *24*, 2945–2986.
- (3) Fujii, M.; Ishikawa, Y.; Ishihara, R.; van der Cingel, J.; Mofrad, M. R.; Horita, M.; Uraoka, Y. Low temperature high-mobility  $\text{InZnO}$  thin-film transistors fabricated by excimer laser annealing. *Appl. Phys. Lett.* **2013**, *102*, 122107 (1–4).

- (4) Zhang, L.; Li, J.; Zhang, X.; Jiang, X.; Zhang, Z. High performance  $\text{ZnO}$ -thin-film transistor with  $\text{Ta}_2\text{O}_5$  dielectrics fabricated at room temperature. *Appl. Phys. Lett.* **2009**, *95*, 072112 (1–3).

- (5) Hwang, Y. H.; Seo, J.-S.; Yun, J. M.; Park, H.; Yang, S.; Park, S.-H. K.; Bae, B.-S. An ‘aqueous route’ for the fabrication of low-temperature-processable oxide flexible transparent thin-film transistors on plastic substrates. *NPG Asia Mater.* **2013**, *5*, e45–e52.

- (6) Park, J. H.; Yoo, Y. B.; Lee, K. H.; Jang, W. S.; Oh, J. Y.; Chae, S. S.; Lee, H. W.; Han, S. W.; Baik, H. K. Boron-doped peroxo-zirconium oxide dielectric for high-performance, low-temperature, solution-processed indium oxide thin-film transistor. *ACS Appl. Mater. Interfaces* **2013**, *5*, 8067–8075.

- (7) Song, K.; Yang, W.; Jung, Y.; Jeong, S.; Moon, J. A solution-processed yttrium oxide gate insulator for high-performance all-solution-processed fully transparent thin film transistors. *J. Mater. Chem.* **2012**, *22*, 21265–21271.

- (8) Banger, K.; Yamashita, Y.; Mori, K.; Peterson, R.; Leedham, T.; Rickard, J.; Siringhaus, H. Low-temperature, high-performance solution-processed metal oxide thin-film transistors formed by a ‘sol-gel on chip’ process. *Nat. Mater.* **2010**, *10*, 45–50.

- (9) Kang, Y. H.; Jeong, S.; Ko, J. M.; Lee, J.-Y.; Choi, Y.; Lee, C.; Cho, S. Y. Two-component solution processing of oxide semiconductors for thin-film transistors via self-combustion reaction. *J. Mater. Chem. C* **2014**, *2*, 4247–4256.

- (10) Su, B.-Y.; Chu, S.-Y.; Juang, Y.-D.; Chen, H.-C. High-performance low-temperature solution-processed  $\text{InGaZnO}$  thin-film transistors via ultraviolet–ozone photo-annealing. *Appl. Phys. Lett.* **2013**, *102*, 192101 (1–4).

- (11) Han, S.-Y.; Herman, G. S.; Chang, C.-H. Low-temperature, high-performance, solution-processed indium oxide thin-film transistors. *J. Am. Chem. Soc.* **2011**, *133*, 5166–5169.

- (12) Meyers, S. T.; Anderson, J. T.; Hung, C. M.; Thompson, J.; Wager, J. F.; Keszi, D. A. Aqueous inorganic inks for low-temperature fabrication of  $\text{ZnO}$  TFTs. *J. Am. Chem. Soc.* **2008**, *130*, 17603–17609.

- (13) Schneller, T.; Waser, R.; Kosec, M.; Payne, D. *Chemical Solution Deposition of Functional Oxide Thin Films*; Springer: Berlin, 2010.

- (14) Choi, K.; Kim, M.; Chang, S.; Oh, T.-Y.; Jeong, S. W.; Ha, H. J.; Ju, B.-K. High-Performance Amorphous Indium Oxide Thin-Film Transistors Fabricated by an Aqueous Solution Process at Low Temperature. *Jpn. J. Appl. Phys.* **2013**, *52*, 060204(1–4).

- (15) Nayak, P. K.; Hedhili, M.; Cha, D.; Alshareef, H. High performance  $\text{In}_2\text{O}_3$  thin film transistors using chemically derived aluminum oxide dielectric. *Appl. Phys. Lett.* **2013**, *103* (033518), 1–5.

- (16) Liu, A.; Liu, G. X.; Shan, F. K.; Zhu, H. H.; Xu, S.; Liu, J. Q.; Shin, B. C.; Lee, W. J. Room-temperature fabrication of ultra-thin  $\text{ZrO}_x$  dielectric for high-performance  $\text{InTiZnO}$  thin-film transistors. *Curr. Appl. Phys.* **2014**, *14*, S39–S43.

- (17) Leppäniemi, J.; Ojanperä, K.; Kololuoma, T.; Huttunen, O.-H.; Dahl, J.; Tuominen, M.; Laukkanen, P.; Majumdar, H.; Alastalo, A. Rapid low-temperature processing of metal-oxide thin film transistors with combined far ultraviolet and thermal annealing. *Appl. Phys. Lett.* **2014**, *105*, 113514 (1–5).

- (18) Rim, Y. S.; Lim, H. S.; Kim, H. J. Low-Temperature Metal-Oxide Thin-Film Transistors Formed by Directly Photopatternable and Combustible Solution Synthesis. *ACS Appl. Mater. Interfaces* **2013**, *5*, 3565–3571.

- (19) Park, J. H.; Kim, K.; Yoo, Y. B.; Park, S. Y.; Lim, K.-H.; Lee, K. H.; Baik, H. K.; Kim, Y. S. Water adsorption effects of nitrate ion coordinated  $\text{Al}_2\text{O}_3$  dielectric for high performance metal-oxide thin-film transistor. *J. Mater. Chem. C* **2013**, *1*, 7166–7174.

- (20) Son, B. G.; Je, S. Y.; Kim, H. J.; Lee, C. K.; Lee, C. K.; Hwang, A. Y.; Won, J. Y.; Song, J. H.; Choi, R.; Jeong, J. K. High-performance  $\text{In-Zn-O}$  thin-film transistors with a soluble processed  $\text{ZrO}_2$  gate insulator. *Phys. Status Solidi (RRL)* **2013**, *7*, 485–488.

- (21) Park, Y. M.; Daniel, J.; Heeney, M.; Salleo, A. Room-Temperature Fabrication of Ultrathin Oxide Gate Dielectrics for Low-Voltage Operation of Organic Field-Effect Transistors. *Adv. Mater.* **2011**, *23*, 971–974.

(22) Park, J. H.; Yoo, Y. B.; Lee, K. H.; Jang, W. S.; Oh, J. Y.; Chae, S. S.; Baik, H. K. Low-Temperature, High-Performance Solution-Processed Thin-Film Transistors with Peroxo-Zirconium Oxide Dielectric. *ACS Appl. Mater. Interfaces* **2013**, *5*, 410–417.

(23) Jeong, S.; Ha, Y. G.; Moon, J.; Facchetti, A.; Marks, T. J. Role of Gallium Doping in Dramatically Lowering Amorphous-Oxide Processing Temperatures for Solution-Derived Indium Zinc Oxide Thin-Film Transistors. *Adv. Mater.* **2010**, *22*, 1346–1350.

(24) Kim, H. S.; Byrne, P. D.; Facchetti, A.; Marks, T. J. High performance solution-processed indium oxide thin-film transistors. *J. Am. Chem. Soc.* **2008**, *130*, 12580–12581.

(25) Barquinha, P.; Martins, R.; Fortunato, E., N-Type Oxide Semiconductor Thin-Film Transistors. *InGaN and ZnO-based Materials and Devices*; Springer: Berlin, 2012; pp 435–476.

(26) Jung, H. Y.; Kang, Y.; Hwang, A. Y.; Lee, C. K.; Han, S.; Kim, D.-H.; Bae, J.-U.; Shin, W.-S.; Jeong, J. K. Origin of the improved mobility and photo-bias stability in a double-channel metal oxide transistor. *Sci. Rep.* **2014**, *4*, 3765–3772.

(27) Jeong, J. K.; Yang, H. W.; Jeong, J. H.; Mo, Y.-G.; Kim, H. D. Origin of threshold voltage instability in indium–gallium–zinc oxide thin film transistors. *Appl. Phys. Lett.* **2008**, *93*, 123508 (1–3).

(28) Pan, T.-M.; Chen, C.-H.; Liu, J.-H.; Her, J.-L.; Koyama, K. Electrical and Reliability Characteristics of High-k  $\text{HoTiO}_3$   $\alpha$ -InGaZnO Thin-Film Transistors. *IEEE Electron Device Lett.* **2014**, *35*, 66–68.

(29) Liu, G. X.; Liu, A.; Shan, F. K.; Meng, Y.; Shin, B. C.; Fortunato, E.; Martins, R. High-performance fully amorphous bilayer metal-oxide thin film transistors using ultra-thin solution-processed  $\text{ZrO}_x$  dielectric. *Appl. Phys. Lett.* **2014**, *105*, 113509 (1–5).